Supplement of

Characteristics of sub-10 nm particle emissions from in-use commercial aircraft observed at Narita International Airport

Nobuyuki Takegawa, et al.

Correspondence to: Nobuyuki Takegawa (takegawa@tmu.ac.jp)

S1 Plume analysis

In the observed air parcels, aircraft emissions from take-off, landing, and idling phases may have been mixed in the atmosphere, and the characterization of particle emissions should be performed carefully. The distance from the observation point to the taxiway was ~380 m and that to the gate was >800 m. We expected that aircraft emissions during idling would contribute to relatively broad, diffuse increases in aerosols and CO_2 and that those during take-off and landing would appear as spiked increases in aerosols and CO_2 at the observation point.

To extract discrete plumes originating from individual aircraft during take-off or landing, we defined background levels for $N_{2.5}$, N_{10}, and CO_2, and calculated enhancements above the background levels ($\Delta N_{2.5}$, ΔN_{10}, and ΔCO_2). The background estimate is more critical for CO_2. For air parcels originating from the runway (wind directions from north to east-southeast, wind speeds of >1 m s^{-1}), the sets of air parcels that were selected by the following procedures were defined as "plumes":

(a) The background air was defined as satisfying the following conditions: $| dCO_2/dt | < 0.1$ ppmv s^{-1}, $| d^2CO_2/dt^2 | < 0.1$ ppmv s^{-2}, $| dN_{10}/dt | < 500$ cm^{-3} s^{-1}, and $N_x < N_{th}$, (x = 2.5 or 10) where d/dt represents the time differential. The second and fourth conditions were set to exclude plume peaks. The threshold value, N_{th}, depends on the meteorological conditions and was set to an appropriate values for each day.

(b) The above background values were interpolated to determine the baselines for $N_{2.5}$, N_{10}, and CO_2. The baseline was subtracted to obtain $\Delta N_{2.5}$, ΔN_{10}, and ΔCO_2.

(c) If the peak ΔCO_2 exceeded 15 ppmv, the ΔCO_2 values decreased below 10% of the peak value within 60 s before or after the peak, and the duration of the enhancement was longer than 30 s, the set of air parcels was selected as "plume".

The above threshold values were determined by considering the observed shapes of CO_2 and aerosol spikes. Step (a) was used to identify "stable" baseline data points, and the conditions were set as redundant. The criterion of 10% in step (c) eliminated overlaps of multiple plumes. This automated procedure may have discarded some possible plume events, depending on the meteorological condition. Nevertheless, we chose these criteria to avoid subjective biases.

Next, the $\Delta N_{2.5}/\Delta CO_2$, $\Delta N_{10}/\Delta CO_2$, and $\Delta N_{10}/\Delta N_{2.5}$ ratios for the identified plumes were calculated. Only data with N_{10} smaller than 5×10^5 cm^{-3} (~1×10^5 cm^{-3} downstream of the dilution section) were used for the analysis because the uncertainty due to particle coincidence increases at higher concentrations. Data obtained on February 15, 16, 20, 21, and 22 were used for the plume analysis. The $\Delta N_{2.5}/\Delta CO_2$, $\Delta N_{10}/\Delta CO_2$, and $\Delta N_{10}/\Delta N_{2.5}$ ratios were calculated by using an area-integration method, similar to that used by Moore et al. (2017a). We also calculated these ratios as linear regression slopes after the data points were averaged over 3 s. The data average was used to account for differences in the response times of the instruments. Although these two methods generally showed reasonable agreement, there were significant discrepancies in some cases, especially at low r^2 values by the regression method. The discrepancy at low r^2 values was because temporal variations in $N_{2.5}$ and N_{10} did not track well with that of CO_2. A possible explanation for this feature is that particle emissions might vary significantly during take-off (e.g., a burst of soot particles in the initial stages), as pointed out by Moore et al. (2017a).

The arrival time of a plume was estimated by considering the wind directions and speeds, assuming that the time for the plume to traverse from the centreline of the runway to the observation point was controlled by the wind vector component perpendicular to the runway. The duration of a plume was estimated from the time difference between the two 10%-crossing points defined in step (c) (when the ΔCO_2 values decreased to below 10% of the peak value within 60 s before or after the peak).

The flight-schedule table provided by NRT, which specified the take-off or landing times of specific aircraft with a time resolution of 1 min, was used to investigate the statistics of aircraft take-offs and landings. During the time periods of the plume analyses, 80–90% of aircraft that passed along the runway were in take-off phases. The flight-schedule table, estimated arrival times, and our video-camera record (only during daytime) were used to attribute the observed plumes to take-off or landing phases. Fig. S1 shows an example of the correspondence between plume events and flight information. Aerosol particle number concentrations for diameters larger than 7 nm (N_7) as measured by the undiluted and unheated CPC 3022 are shown for comparison. In Fig. S1a, we can see a reasonably good agreement between N_7 and N_{10}, as expected. In Fig. S1b, depletion of aerosol particle number concentrations upon heating is evidently found.

Although the observed plumes could, in most cases, be attributed to take-off or landing of specific aircraft, there were some cases in which the one-to-one correspondence was somewhat ambiguous (shown as “unidentified” in Fig S1a). We attributed 132 plumes to take-offs for the unheated mode and 63 plumes to the 350°C-heated mode. Potential uncertainties in the attribution (i.e., a landing plume incorrectly assigned to a take-off plume) are 10–20% at most, considering that 80–90% of aircraft that passed along the runway were in take-off phases. Table S1 shows the statistical summary of particle number EIs classified by major aircraft models identified in this study. We did not observe significant difference in the particle number EIs among these models, although there might be uncertainties in the attribution, as mentioned above.

Fig. S2 shows histograms of estimated arrival time and duration of plumes. Although our sampling conditions differed from those given by Moore et al. (2017a), the estimated arrival duration times were comparable to their values. We did not find systematic dependence of the $\Delta N_{10}/\Delta CO_2$ and $\Delta N_{2.5}/\Delta CO_2$ ratios on the arrival time of plumes, as indicated in Fig. S3.

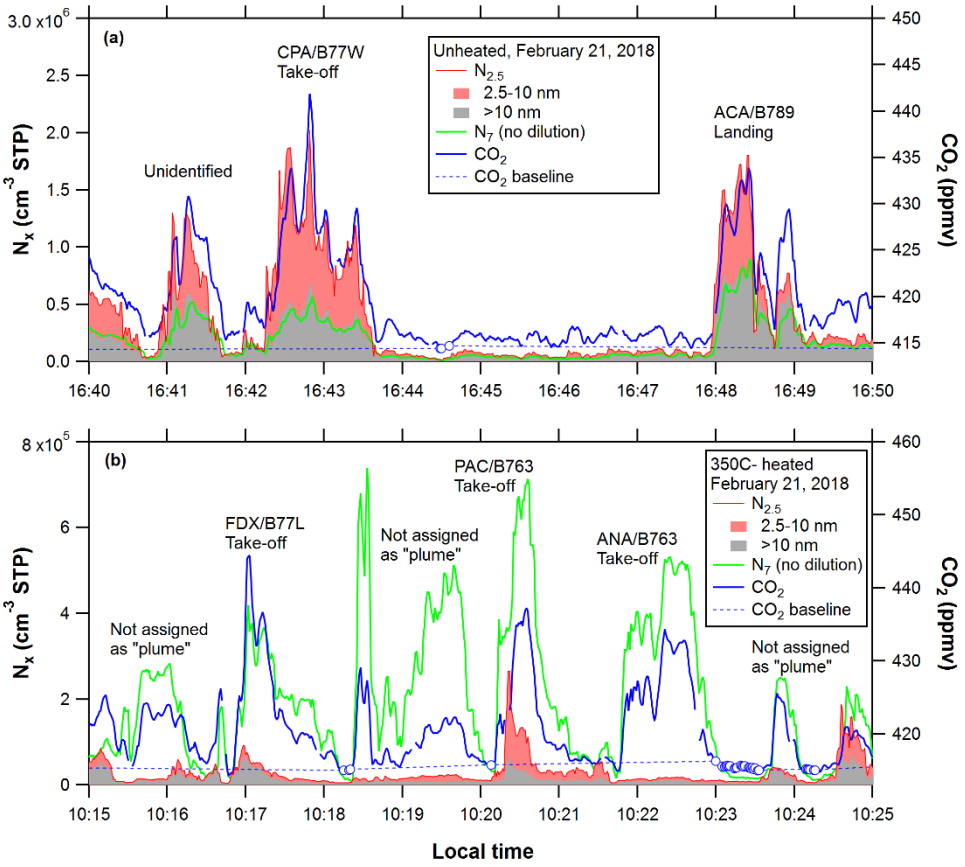

65 **Figure S1:** Examples of discrete plumes. Data for (a) unheated and (b) 350°C-heated mode observed on February 21, 2018 are shown. Slight differences in the peak timing for very sharp spikes may be affected by instrument response times. The blue open circles represent estimated "background" concentrations for CO_2, and the blue dashed lines represent the interpolated background levels.

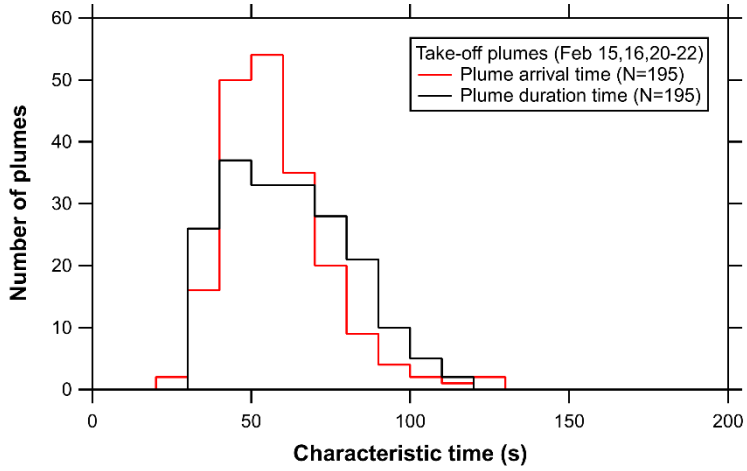

Figure S2: Histograms of the estimated arrival time and duration of plumes. The lower and upper limits of the duration time (30 s and 120 s, respectively) were determined by the definition of plumes.

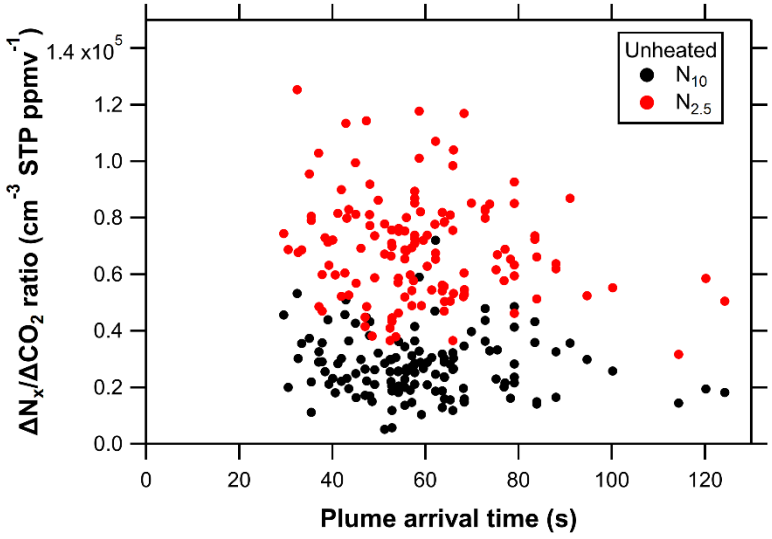

Figure S3: Dependence of $\Delta N_{2.5}/\Delta CO_2$ and $\Delta N_{10}/\Delta CO_2$ ratios on the arrival time of plumes.

Table S1: Medians of particle number EIs for take-off plumes classified by major aircraft models identified in this study (the number of samples ≥ 5). The unit of particle number EIs is 10^{15} kg-fuel^{-1}.

Aircraft model	Total				Non-volatile			
	Number of samples	EI($N_{2.5}$)	EI(N_{10})	Sub-10 nm fraction	Number of samples	EI($N_{2.5}$)	EI(N_{10})	Sub-10 nm fraction
A320	12	80	44	0.44	N/A	N/A	N/A	N/A
A321	N/A	N/A	N/A	N/A	6	3.6	2.3	0.44
A333	21	94	35	0.65	9	2.4	1.2	0.49
B738	9	117	45	0.56	N/A	N/A	N/A	N/A
B748	5	114	41	0.66	N/A	N/A	N/A	N/A
B763	14	129	50	0.64	11	9.4	1.8	0.66
B772	7	91	26	0.71	N/A	N/A	N/A	N/A
B77W	15	96	34	0.65	9	2.7	1.3	0.49
B788	10	139	71	0.54	N/A	N/A	N/A	N/A
B789	12	125	64	0.54	N/A	N/A	N/A	N/A